

Prediction of Turbulent Thermal Boundary Layers Using Scalar Turbulence Modeling Techniques

M.D. EL HAYEK
Mechanical Engineering Department
Notre Dame University - Louaize
P.O.Box 72 / Zouk-Mikael
LEBANON
mhayek@ndu.edu.lb

Abstract: The present investigation deals with the development of advanced scalar turbulence modeling approaches and their application to the calculation of non-isothermal wall-bounded flow phenomena. A new scalar modeling technique based on scalar turbulent scales is proposed and implemented at a second-order modeling approach. Instead of the classical analogy concept between the mechanical and the scalar transport mechanisms, a scalar time scale, defined as the ratio of the temperature variance and its rate of dissipation or scalar dissipation rate, is used to tackle the scalar turbulence closure problem. At the level of second-order modeling technique, the scalar scales are directly used to derive relationships for the different unknown correlations like the turbulent diffusion, the pressure-temperature gradient correlation, etc. The result is a very simple scalar Reynolds stress model capable of predicting various heat transport problems. Such a new modeling approach is compared with its standard mechanical counterpart as well as first-order models like the k - ϵ model and the g - χ model, a scalar version of the standard k - ϵ . Validation against experimental data is performed and shows clearly the benefits of adopting the right scale for the right phenomenon: mechanical scales for momentum transport and specific scalar scales for scalar transport.

Key-Words: Turbulence Scales, Turbulence Models, Wall Function, Convective Heat Transfer, Thermal Boundary Layer, Turbulent Prandtl Number.

1 Introduction

The turbulent wall-bounded flows are largely encountered in engineering applications involving heat or mass transfer. The prediction of such problems requires the implementation of robust numerical techniques to solve the partial differential equations governing the transport mechanisms. Furthermore, advanced turbulence closure techniques are needed to correctly model the combination of features encountered in such flows, the most critical being the thermal boundary layer and its development along walls. Engineering turbulence closures or models are usually based on a scale reduction technique in which the flow phenomenon under investigation is described by one or two scales at most down from infinity.

Many turbulence models have been developed, ranging from the simplest or the mixing length model to advanced approaches like Reynolds stress model (RSM), Large Eddy Simulation (LES), etc.... Despite their wide use for general engineering applications, these models still show many discrepancies when applied to wall dominated flows. The causes are multiple: near-wall features,

high Reynolds models, etc. All these causes are addressed in the literature by using artificial damping functions to force the models to become compatible with the vanishing turbulence intensity in the near-wall zone. Many so-called low-Reynolds number models have been developed and are used for specific applications, especially for convective heat transfer calculations. None of these models can be, however, considered as universal. The problem is even worst when dealing with the scalar transport since for such phenomenon, additional difficulties have to be addressed prior to using the resulting models. One of such difficulties is the largely used analogy concept, which appears at nearly all modeling levels: directly in the two-equation models through the use of the constant turbulent Prandtl number hypothesis and implicitly in the second order closures by using similar turbulence scales for momentum and heat transport mechanisms. The strong anisotropy of the turbulent fluxes is another non-negligible feature characterizing the turbulent transport of heat and/or species and should be taken into account when developing specific models for the scalar transport problem.

The analogy problem has been addressed in earlier investigations at different modeling levels [1-6]. The main idea was to represent each flow phenomenon by its own scales: the hydrodynamics by the standard mechanical time scale (k/ε) and the scalar transport by a specific scalar time scale instead of the same ratio k/ε . Several choices may be considered for the scalar time scale but a natural choice, further supported by experimental facts, seems to be the ratio of the variance of temperature over its scalar rate of dissipation, g/χ , [3]. Such a change from k/ε to g/χ in modeling the scalar transport mechanism proved to be highly beneficial. The use of scalar scales along with the classical mechanical ones is more and more encountered in the literature.

The anisotropy can be naturally accommodated by using an appropriate Reynolds stress closure. Of this latter kind, the present study adopts the standard model for its more universal nature [7]. The standard Reynolds stress model was then extended by using an appropriate scalar time scale to close the turbulent flux equations in a manner similar to that adopted for the two-equation model [3]. The time scale g/χ is used to model the different terms that require modeling in the turbulent flux equations. The result is a new kind of simple engineering scalar Reynolds stress model (SRSM), which has to be compared with more sophisticated Reynolds stress models and their cumbersome algebraic treatment like the cubic model [8].

Another important point to be considered in the present study concerns the numerical technique and its implementation. Of special importance are the boundary conditions, especially the conditions prevailing in the near wall zones. In this respect, the classical wall function approach is adopted and extended to the scalar turbulence parameters. In spite of their shortcomings, wall functions remain the best solution for flows of engineering interest [9-10]. A special two-layer scalar wall function is developed for the new scalar turbulence quantities and is used along with the standard two-layer wall function for the flow. The numerical technique is the standard finite volumes technique with staggered grid and standard numerical schemes.

The advantages and disadvantages of the different turbulence models are discussed in light of comparisons with experimental data. The results show clearly the benefits of the scalar modeling approach and its promising features when dealing with wall bounded flows. Similar improvements were obtained in previous investigations considering free flow phenomena [5].

2 Governing Equations

The most appropriate equations to describe flow fields are the classical Navier-Stokes equations. For constant-density turbulent flows, however, and as a result of the complex nature of such flows, a more practical representation is generally considered especially when dealing with engineering problems. It consists of the Reynolds averaged Navier-Stokes (RANS) equations given by

$$\frac{\partial \rho U_j}{\partial x_j} = 0 \quad (1)$$

$$\frac{\partial \rho U_j U_i}{\partial x_j} = \frac{\partial}{\partial x_j} \left[\mu \frac{\partial U_i}{\partial x_j} - \rho \overline{u_i u_j} \right] - \frac{\partial P}{\partial x_i} \quad (2)$$

$$\frac{\partial \rho c_p U_j T}{\partial x_j} = \frac{\partial}{\partial x_j} \left[k \frac{\partial T}{\partial x_j} - \rho c_p \overline{u_j t} \right] + S_\theta \quad (3)$$

and representing the conservation of mass, momentum along the different space directions, and energy. The main problem with such transformed equations is the fact that they involve more unknowns than equations. An appropriate closure method is required in order to close the set under consideration. Usually turbulence models in more or less elaborate forms are used to determine the statistical second-order moments, namely, the Reynolds stresses and the turbulent heat fluxes.

3 Turbulence Modeling

Many turbulence models have been developed and are widely used, with more or less success, to predict different kinds of engineering turbulent flows. Most of these models address mainly the mechanical aspect of the problem, e.g., the closure of the momentum equation. The heat transport aspect is generally handled by invoking some analogy concepts between the transport of momentum and heat. Experiments show however, that the analogy can be used only in limited cases (Prandtl number very close to unity). A completely different approach is needed for the heat transport problem or the transport of any scalar quantity in general. The main idea behind such a new modeling technique is to make each phenomenon governed by its own scales. The hydrodynamic aspect will continue to be characterized by the same mechanical scales: the turbulent kinetic energy, its dissipation rate and their derivatives. The transport of heat or the mixing mechanism is to be characterized by a set of scalar scales. To this end, the variance of temperature, g , and its rate of dissipation, χ , or scalar dissipation rate, are used.

The second order modeling approach used to naturally tackle the anisotropy of the turbulent fluxes is based on the fact that all the statistical unknowns appearing in the RANS equations (1-3) are governed by their transport equations

$$\frac{\partial \rho U_k \overline{u_i u_j}}{\partial x_k} = D_{ij} + P_{ij} + \Phi_{ij} - \frac{2}{3} \rho \varepsilon \delta_{ij} \quad (4)$$

$$\frac{\partial \rho U_k \overline{u_i t}}{\partial x_k} = D_{i\theta} + P_{i\theta} + \Phi_{i\theta} \quad (5)$$

where P_{ij} and $P_{i\theta}$ represent the generation by mean fields given by

$$P_{ij} = -\overline{\rho u_i u_k} \frac{\partial U_j}{\partial x_k} - \overline{\rho u_j u_k} \frac{\partial U_i}{\partial x_k} \quad (6)$$

$$P_{i\theta} = P_{i\theta 1} + P_{i\theta 2} = -\overline{\rho u_i u_j} \frac{\partial T}{\partial x_j} - \overline{\rho u_j t} \frac{\partial U_i}{\partial x_j} \quad (7)$$

D_{ij} and $D_{i\theta}$ are the diffusion terms generally modeled using the generalized gradient diffusion hypothesis

$$D_{ij} = \frac{\partial}{\partial x_k} \left(C_c \tau_c \overline{\rho u_k u_i} \frac{\partial \overline{u_i u_j}}{\partial x_1} \right) \quad (8)$$

$$D_{i\theta} = \frac{\partial}{\partial x_k} \left(C_\theta \tau_\theta \overline{\rho u_k u_i} \frac{\partial \overline{u_i t}}{\partial x_1} \right) \quad (9)$$

where τ_c and τ_θ are the appropriate time scales characterizing the corresponding diffusion mechanisms. In the standard Reynolds stress model (RSM), the analogy is taken for granted and τ_θ is set equal to τ_c , i.e. k/ε . The present investigation (SRSM) considers each diffusion phenomenon to be governed by its own scale. The scalar time scale needed is given by

$$\tau_\theta = g/\chi \quad (10)$$

The next two terms or the pressure-strain correlation, Φ_{ij} , and the pressure-temperature gradient correlation, $\Phi_{i\theta}$, are the most important due to their role in distributing the turbulent energy between the different stresses and fluxes. The modeling of these terms was and still is the most debated aspect of the second order modeling approach. In the frame of the standard Reynolds stress model, they are modeled as the superposition of two effects: the slow part or turbulence-turbulence interaction and the rapid part or the mean strain-turbulence interaction.

$$\Phi_{ij} = \Phi_{ij}^{(1)} + \Phi_{ij}^{(2)} + \Phi_{ijw}^{(1)} + \Phi_{ijw}^{(2)} \quad (11)$$

where $\Phi_{ij}^{(1)}$ and $\Phi_{ij}^{(2)}$ are modeled using the "return to isotropy" and the "isotropization of production" models [7], respectively,

$$\Phi_{ij}^{(1)} = -C_1 (\overline{\rho u_i u_j} - 2\rho k \delta_{ij} / 3) / \tau_c \quad (12)$$

$$\Phi_{ij}^{(2)} = -C_2 (P_{ij} - P_{kk} \delta_{ij} / 3) \quad (13)$$

and $\Phi_{ijw}^{(1)}$ and $\Phi_{ijw}^{(2)}$ are modeled using the standard wall reflection models

$$\Phi_{ijw}^{(1)} = C_{1w} \frac{\rho}{\tau_c} \left(\overline{u_k u_i n_k n_j} \delta_{ij} - \frac{3}{2} \overline{u_i u_k n_j n_k} - \frac{3}{2} \overline{u_j u_k n_i n_k} \right) F_\alpha(x_n) \quad (14)$$

$$\Phi_{ijw}^{(2)} = C_{2w} \left(\Phi_{kl}^{(2)} n_k n_l \delta_{ij} - \frac{3}{2} \Phi_{ik}^{(2)} n_j n_k - \frac{3}{2} \Phi_{jk}^{(2)} n_i n_k \right) F_\alpha(x_n) \quad (15)$$

F_α is a function of the normal distance to the wall, x_n , used to damp the contribution of the wall terms in the pressure-strain correlation in the core of the flow. In the present study, an enhanced form is proposed and used instead of the classical form [3].

$$F_\alpha(x_n) = \text{MIN} \left(\frac{C_\mu^{-1/4} (\overline{uv})^2}{\kappa k^{1/2} \varepsilon x_n}, \frac{C_\mu^{3/4} k^{3/2}}{\kappa \varepsilon x_n} \right) \quad (16)$$

Similar treatment of the turbulent heat fluxes allows the pressure-temperature gradient correlation to be written as

$$\Phi_{i\theta} = \Phi_{i\theta}^{(1)} + \Phi_{i\theta}^{(2)} + \Phi_{i\theta w}^{(1)} + \Phi_{i\theta w}^{(2)} \quad (17)$$

where the different components, $\Phi_{i\theta}^{(1)}$, $\Phi_{i\theta}^{(2)}$, $\Phi_{i\theta w}^{(1)}$, and $\Phi_{i\theta w}^{(2)}$ are modeled using the following relationships

$$\Phi_{i\theta}^{(1)} = -C_{1\theta} \overline{\rho u_i t} / \tau_\theta \quad (18)$$

$$\Phi_{i\theta}^{(2)} = -C_{2\theta} P_{i\theta 2} \quad (19)$$

$$\Phi_{i\theta w}^{(1)} = -\left(C_{1\theta w} \overline{\rho u_k t n_i n_k} / \tau_\theta \right) F_\alpha(x_n) \quad (20)$$

$$\Phi_{i\theta w}^{(2)} = C_{2\theta w} \Phi_{k\theta}^{(2)} n_i n_k F_\alpha(x_n) \quad (21)$$

The last term of equation (4) represents the dissipation mechanism as modeled using the hypothesis of isotropic small scales. The mechanical dissipation rate is determined using a transport-like equation

$$\frac{\partial \rho U_j \varepsilon}{\partial x_j} = \frac{\partial}{\partial x_j} \left[C_\varepsilon \frac{k}{\varepsilon} \overline{\rho u_j u_k} \frac{\partial \varepsilon}{\partial x_k} \right] + \frac{\varepsilon}{k} (C_{\varepsilon 1} P_{kk} - C_{\varepsilon 2} \rho \varepsilon) \quad (22)$$

The application of the same hypothesis to the turbulent fluxes leads to a null dissipation term as shown in equation (5).

The set of constants used in the standard Reynolds stress model is given in tables 1a and 1b.

Table 1a. Mechanical constants of the standard RSM.

C_c	C_1	C_2	C_{1w}	C_{2w}	C_ε	$C_{\varepsilon 1}$	$C_{\varepsilon 2}$
0.22	1.8	0.6	0.5	0.3	0.18	1.44	1.92

Table 1b. Scalar constants of the standard RSM.

C_θ	$C_{1\theta}$	$C_{2\theta}$	$C_{1\theta w}$	$C_{2\theta w}$
0.2	3.0	0.5	0.5	0.0

The different constants involved in the SRSM model can be determined using simple flow cases for which experimental data are available. Here a simple identification procedure with the standard model constants, in conjunction with a constant time

scale ratio hypothesis, is used to determine them. Numerical tuning is then performed and the resulting set is given in table 2. Comparison of these values with their mechanical counterparts (table 1a) shows the good equivalence between the two sets. This means that the same constants may be used for different phenomena provided that the right scales are adopted.

Table 2. Scalar constants of the SRSM.

C_θ	$C_{1\theta}$	$C_{2\theta}$	$C_{1\theta w}$	$C_{2\theta w}$
0.2	2.0	0.5	0.2	0.0

To complete the modeling procedure, additional means are needed to evaluate the scalar time scale components, g and χ . Like their mechanical counterparts, g and χ are evaluated using transport-like equations resulting from the energy conservation equation using suitable algebraic and averaging techniques. After the necessary second order modeling, the governing equations become [3]

$$\frac{\partial \rho U_j g}{\partial x_j} = \frac{\partial}{\partial x_j} \left[C_g \tau_{\theta 0} \overline{\rho u_j u_k} \frac{\partial g}{\partial x_k} \right] + P_g - \rho \chi \quad (23)$$

$$\frac{\partial \rho U_j \chi}{\partial x_j} = \frac{\partial}{\partial x_j} \left[C_\chi \tau_{\theta 0} \overline{\rho u_j u_k} \frac{\partial \chi}{\partial x_k} \right] + \frac{\chi}{g} (C_{\chi 1} P_g - C_{\chi 3} \rho \chi) + \frac{\chi}{k} \left(C_{\chi 2} \frac{P_{kk}}{2} - C_{\chi 4} \rho \epsilon \right) \quad (24)$$

where P_g is the production terms of the temperature variance by the mean flow field giving by

$$P_g = -\rho u_j t \frac{\partial T}{\partial x_j} \quad (25)$$

Here too, the different constants can be determined using simple flow fields for which it is possible to simplify the governing equations and then solve them analytically. The following set of constants results from such an initial evaluation process

$$\begin{aligned} C_{\chi 1} &= 1.0 & C_{\chi 2} &= C_{\epsilon 1} - 1 = 0.44 \\ C_{\chi 3} &= R(C_{\epsilon 2} - 1) & C_{\chi 4} &= 1/R \\ \sigma_g &\approx 1.0 & \sigma_\chi &= \frac{C_\mu^{1/2} \kappa_\theta^2}{C_\alpha C_{\chi 3} - C_{\chi 1} + R(C_{\chi 4} - C_{\chi 2})} \end{aligned} \quad (26)$$

where κ_θ is the inverse of the slope of the temperature law of the wall and R the time scale ratio (τ_θ/τ_c). The constant C_g is directly obtained from experimental results. The resulting values are then further refined by numerical tuning to reach the set given in table 3.

Table 3. Constants for the g - χ equations.

C_g	C_χ	σ_g	σ_χ	$C_{\chi 1}$	$C_{\chi 2}$	$C_{\chi 3}$	$C_{\chi 4}$
0.2	0.2	1.0	1.0	1.0	0.44	1.12	0.82

It is worth mentioning that the scalar scales are usually incorporated automatically into advanced second order modeling approaches [8]. By doing so, an implicit recognition of the fact that the scalar fields should be governed in a way or another by their own scales is formulated. The present study develops such an idea to its fullest extent while trying to keep the models as simple as possible.

4 Near-Wall Model

In wall-bounded flows, the assumption of high Reynolds numbers ceases to be valid in the near wall zones where the viscous forces become non-negligible. Special treatment is required to solve the near-wall behavior. The most general approach is to modify the models in order to take into account the specific features of the near wall zone. Many models have been developed in this respect and unfortunately, none can be considered universal. Moreover, such models require generally very fine meshes near the walls, a requirement that is very expensive when considering flow and heat transfer problems of engineering interest.

Owing to that, a simpler approach is often recommended, especially when considering flows of engineering interest where the resolution of the near-wall zones becomes an obstacle [9-10]. It consists of advanced wall function techniques used to jump over the near-wall zone from the wall itself to the turbulent layer. In the present study, the classical two-layer wall function is used for the flow and a scalar version is developed and used to represent the behavior of the scalar transport in the near wall region [3]. A brief description is given here for the scalar two-layer wall function.

The basic law behind the wall function is the law of the wall for the temperature [11]

$$T^+ = \frac{T_w - T}{T_\phi} = \frac{1}{\kappa_\theta} \ln(\text{Pr} y^+) + (3.85 \text{Pr}^{1/3} - 1.3)^2 \quad (27)$$

in which κ_θ is generally function of the value of the turbulent Prandtl number at the wall. T_ϕ is the “friction” or flux temperature.

It is to be noticed that this law is not as universal as the similar law for the velocity but it is a convenient tool for practical engineering flow fields with heat transfer. The wall turbulent Prandtl number is often assumed to be constant for a wide range of molecular Prandtl number [12]. Departure from such a universal behavior is noticed however for very small Prandtl number.

Like for the flow wall function, the scalar wall function divides the near wall zone into two layers: an inner layer where the conduction mechanism is

dominant and an outer layer where the convection takes over. Such a division is represented schematically in figure 1.

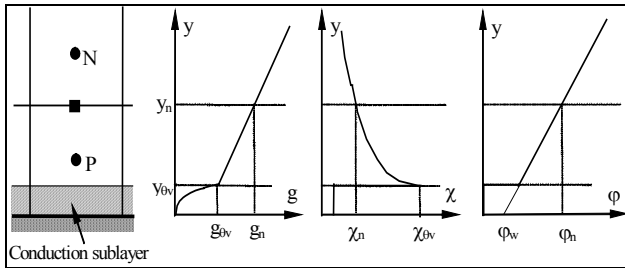


Fig.1 Two-layer scalar wall function.

The thickness of the conduction sublayer can be related to its viscous counterpart using the molecular Prandtl number by

$$y_{\theta v} = y_v / Pr^a \tag{28}$$

in which the exponent, a , of the Prandtl number is around 0.5, [13], and y_v is the dimensionless distance to the wall used to define the viscous sublayer and given by

$$Re_v = \rho y_v k_v^{1/2} / \mu = 20 \tag{29}$$

Assumptions are then made concerning the variation of the different turbulence quantities in both the conduction sublayer and the outer turbulent layer as shown in figure 1 [3]. The resulting relationships are used to evaluate the different gradients normal to the wall in the governing equations of the turbulent fluxes and the scalar time scale. Typical result for the production term of the variance of temperature is given by

$$\overline{P_g} = \frac{1}{\rho C_\mu^{1/4} \kappa_\theta k_v^{1/2} y_n} \left(\frac{\phi_w}{c_p} \right)^2 \ln \left(\frac{y_n}{y_{\theta v}} \right) \tag{30}$$

where ϕ_w is the heat flux at the wall. Similar relationships can be obtained for the remaining terms in the other equations involving the same gradient of temperature. As for the scalar dissipation rate, the following simple analytical solution is used to evaluate its value in the first cell near the wall

$$\chi = \frac{2g_{\theta v}}{y_{\theta v} y_n} + \frac{C_\alpha g_{\theta v} k_v^{1/2}}{\kappa_\theta C_\mu^{1/4} y_n} \ln \left(\frac{y_n}{y_{\theta v}} \right) \tag{31}$$

5 Numerical Technique

The various turbulence models have been implemented into a computational fluid dynamics code. The finite volumes method is used with different algorithms to handle the pressure-velocity coupling and several differencing schemes to discretize the convective transport terms. The SIMPLEC algorithm is used in the present study along with a power law scheme.

6 Thermal Boundary Layer

The whole procedure is used to predict the hydrodynamics as well as the thermal behavior of a turbulent boundary layer flow developing along a flat plate subjected to a sudden change of surface heat flux [13]. The geometry is a flat plate 3.9m long subjected to a heat flux of 270 W/m² over the last 2.4m of its length (thermal boundary layer starts at $X_0=1.5m$). Air at $T_0=26^\circ C$ is blown over the plate at a velocity of 9.45 m/s. The non-uniform staggered mesh used consists of 220x75 control volumes along the streamwise and transversal directions, respectively. Numerical tests were carried out to ensure that the mesh is fine enough to result in a mesh independent solution without violating the requirements of the wall boundary conditions.

One generally and widely used criterion to check the validity of numerical techniques is the overall heat transfer coefficient represented here by the Stanton number as sketched in figure 2. Here the results of the two second-order models (RSM and SRSM) are compared with experimental results. The results obtained with the standard $k-\epsilon$ and a scalar version, the $g-\chi$ model, are also represented for information. The superior performance of the scalar models appears clearly although the mechanical models perform not bad. Such very good agreement is due mainly to the better predictions obtained with the scalar models concerning the temperature distribution across the boundary layer as shown in figure 3 at two different locations along the streamwise direction; X^* being the streamwise distance from the entrance of the heated zone normalized by the boundary layer thickness at that entrance. Here the better representation of the thermal boundary layer development is shown since the scalar models perform much better at an earlier stage in the development process (figure 3a).

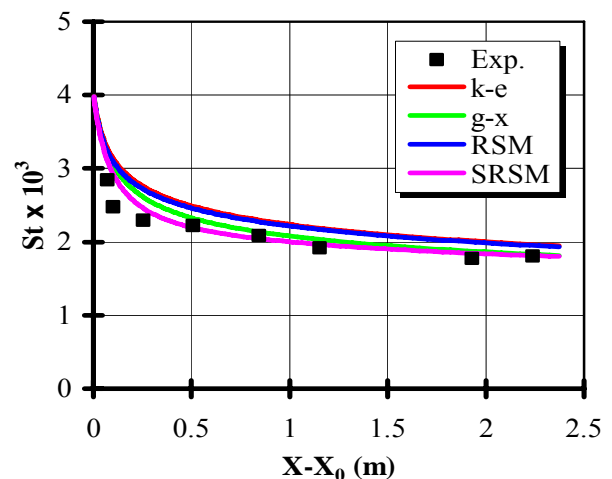


Fig.2. Stanton number along the plate.

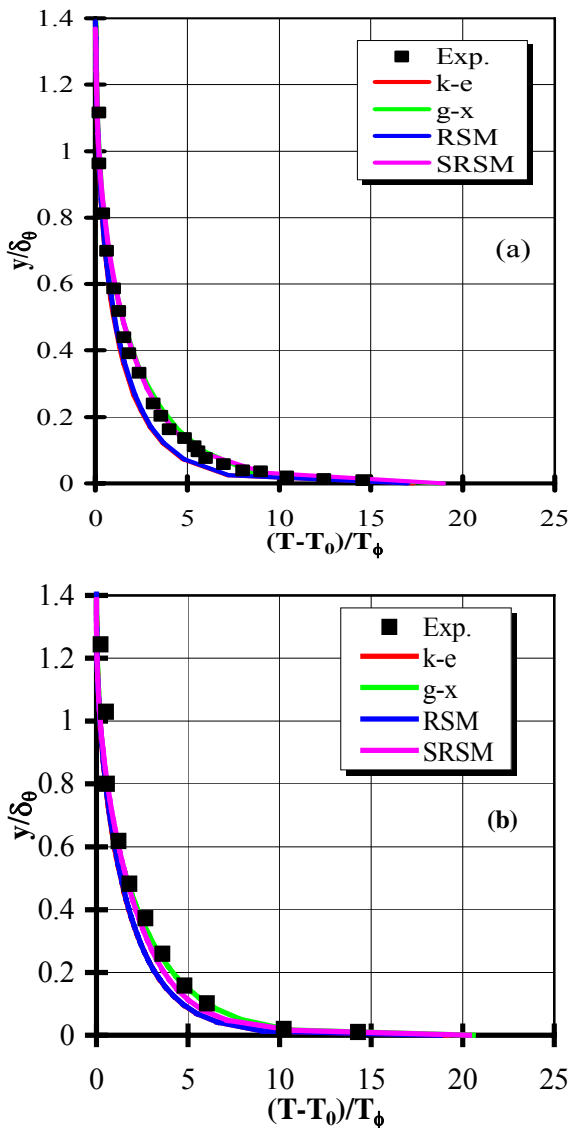


Fig.3 Mean temperature across the boundary layer, (a): $X^*=18.9$, and (b): $X^*=42.9$.

The transversal turbulent fluxes are shown in figure 4 where similar results are obtained by all the models of both first and second orders, mechanical and scalar forms. This is something usual since most models are tuned to predict correctly the behavior of the transversal turbulent heat flux across the boundary layer. The SRSM seems to predict slightly higher values than the other models but the results remain within the error margins of the experimental data.

Figure 5 shows the streamwise heat flux represented by its ratio to the transversal heat flux. Here too, the SRSM seems to be better, especially in the early development phase. The first order models, $k-\epsilon$ and $g-\chi$, are not represented in this figure due to the simple fact that they cannot predict the streamwise flux at all; a shortcoming common to all first order models used nowadays.

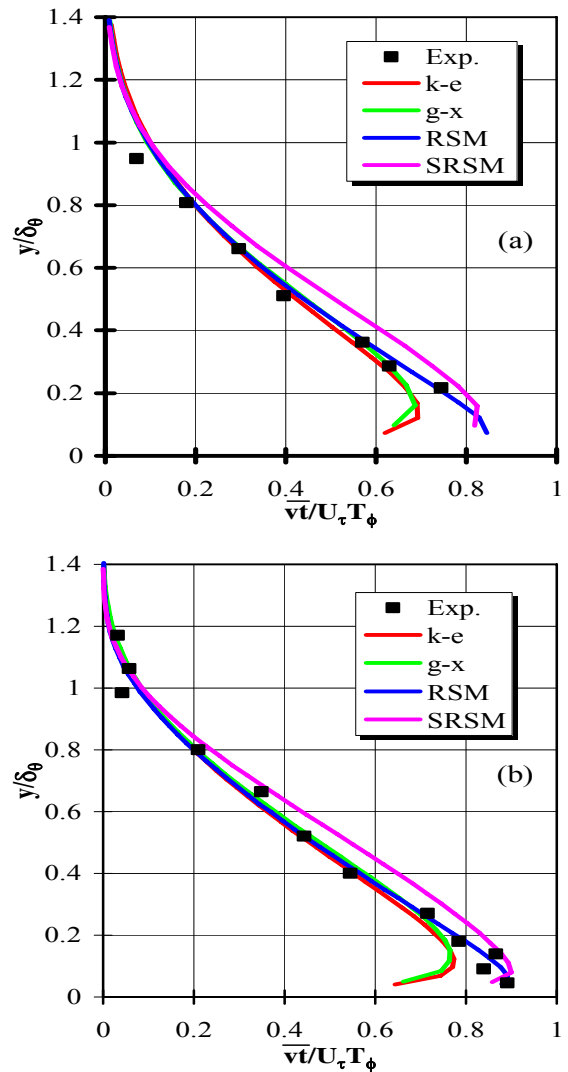


Fig.4 Transversal turbulent heat flux across the boundary layer, (a): $X^*=18.9$, and (b): $X^*=42.9$.

The predicted temperature fluctuations are compared in figure 6 with the corresponding experimental data. Here, obviously, the scalar models are shown only. The comparison between experiment and predictions is in favor of the $g-\chi$ model. It means that the SRSM should be further tuned or improved in order to match correctly the experimental results.

Figure 7 shows the distribution of the turbulent Prandtl number across the boundary layer. As it is clear, all the models fail to predict correctly Pr_t . The scalar models seem, however, better than the mechanical ones in such a way that they predict a variable Pr_t and not a nearly constant as with the mechanical models (by assumption). It is important to notice the ability of the scalar models to predict an increasing turbulent Prandtl number versus the distance to the wall in agreement with experimental data and analytical studies [14-15]. This is especially true far downstream where the two

boundary layers, hydrodynamic and thermal, reach a steady development phase.

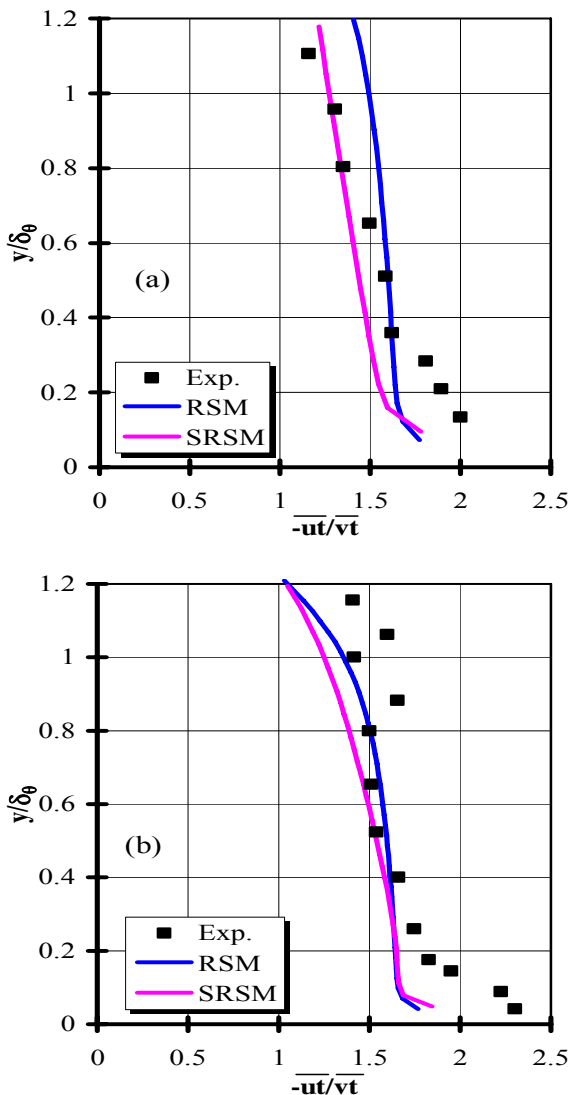


Fig.5 Ratio of turbulent heat fluxes across the boundary layer, (a): $X^*=18.9$, and (b): $X^*=42.9$.

A last result concerns the time scale ratio, which is most often assumed to be a constant of nearly 0.5 in the literature. Figure 8 compares the prediction of the scalar models with the experimental results of Verriopoulos as given in [1], for a thermal boundary layer developing from the leading edge of the plate in parallel to the hydrodynamic boundary layer. The models predict variable time scale ratio with an average value of the same order of magnitude as the experimental results. Like for the turbulent Prandtl number, it should be noted here that the measurement of such a parameter is impossible directly and must be calculated from other experimental data, thus amplifying possible experimental errors.

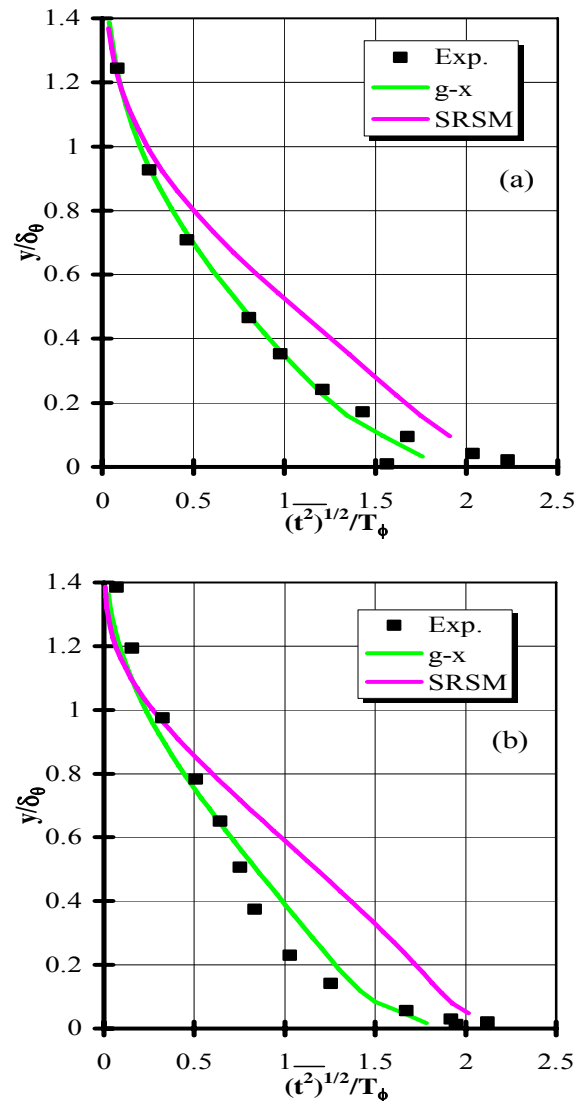


Fig.6 Temperature fluctuations across the boundary layer, (a): $X^*=18.9$, and (b): $X^*=42.9$.

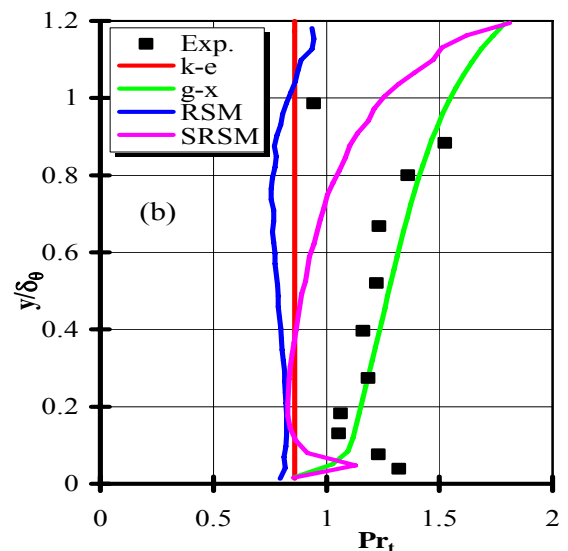


Fig.7 Turbulent Prandtl number across the boundary layer, $X^*=42.9$.

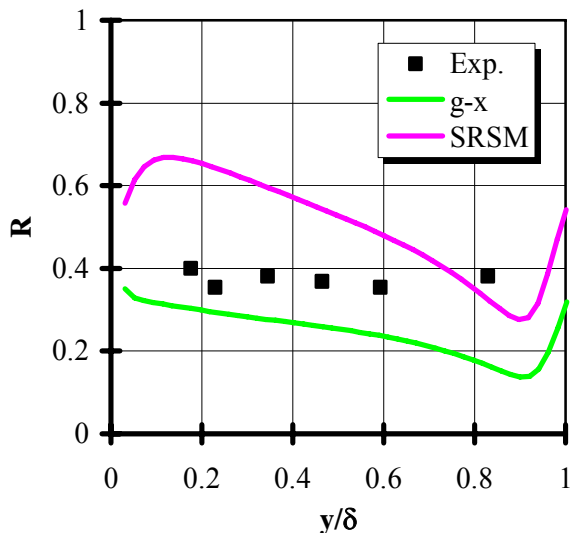


Fig.8 Time scale ratio across a thermal boundary layer.

7 Conclusion

As a conclusion, the present scalar modeling approaches achieve generally better prediction than their standard mechanical counterparts. The usually assumed constant parameters like the turbulent Prandtl number and the time scale ratio are not constant and their variations must be taken into account even for simple flow fields like the thermal boundary layer developing in turbulent regime over a flat plate as considered in the present study.

Advanced modeling approaches involving very complicated mathematics are not always the panacea. Simpler scalar modeling approaches as presented here seem to be an attractive alternative owing to their simplicity. Of course, two supplementary equations have to be solved. This can, however, be achieved at very small cost since the extra CPU time required is almost negligible. Furthermore, the scalar models deliver naturally additional quantities that may be needed in some applications in which the temperature fluctuations are critical design parameters.

References:

- [1] Y. Nagano, C. Kim, A Two-Equation Model for Heat Transport in Wall Turbulent Shear Flows, *ASME - Journal of Heat Transfer*, Vol.110, 1988, pp.583-589.
- [2] R.M.C. So, T.P. Sommer, A Near-Wall Eddy Conductivity Model for Fluids with Different Prandtl Numbers, *ASME - Journal of Heat Transfer*, Vol.116, 1994, pp.844-854.
- [3] M. El Hayek, *Le transfert de chaleur par convection en régime turbulent: aspects physiques et numériques*, Thèse de Doctorat Européen, Faculté Polytechnique de Mons, Mons (Belgium), 1997.
- [4] C.B. Hwang, C.A. Lin, A Low Reynolds Number Two-Equation k_θ - ε_θ model to predict thermal fields, *International Journal of Heat and Mass Transfer*, Vol.42, 1999, pp.3217-3230.
- [5] M. El Hayek, Prediction of Heated Turbulent Jet Flow using Advanced Scalar Turbulence Models", paper IMEC2004-3002 in Proceedings of IMEC2004 "Recent Advances and Applications in Fluid Mechanics", Part I, Kuwait Society of Engineers, 2004, pp.15-32.
- [6] M. Karcz, J. Badur, An alternative Two-Equation Turbulent Heat Diffusivity Closure, *International Journal of Heat and Mass Transfer*, Vol.48, 2005, pp.2013-2022.
- [7] B.E. Launder, G.J. Reece, W. Rodi, Progress in the Development of a Reynolds-Stress Turbulence Closure, *Journal of Fluid Mechanics*, Vol.68, 1975, pp.537-566.
- [8] T.J. Craft, *Second-Moment Modelling of Turbulent Scalar Transport*, Ph.D. Thesis, University of Manchester Institute of Science and Technology (UK), 1991.
- [9] T.J. Craft, S.E. Gant, A.V. Gerasimov, H. Iacovides, B.E. Launer, Development and Application of Wall-Function Treatments for Turbulent Forced and Mixed Convection Flows, *Fluid Dynamics Research*, Vol.38, 2006, pp.127-144.
- [10] G. Kalitzin, G. Medic, G. Iaccarino, P. Durbin, Near-Wall Behavior of RANS Turbulence Models and Implementations for Wall Functions, *Journal of Computational Physics*, Vol.204, 2005, pp.265-291.
- [11] B.A. Kader, Temperature and Concentration Profiles in Fully Turbulent Boundary Layers, *International Journal of Heat and Mass Transfer*, Vol.24, 1981, pp.1541-1544.
- [12] V.S. Arpaci, P.S. Larsen, *Convection Heat Transfer*, Prentice-Hall (USA), 1984.
- [13] R.A. Antonia, H.Q. Danh, A. Prabhu, Response of Turbulent Boundary Layer to a Step Change in Surface Heat Flux, *Journal of Fluid Mechanics*, Vol.80, 1977, pp.153-177.
- [14] W.M. Kays, Turbulent Prandtl Number - Where Are We?, *Transactions of the ASME - Journal of Heat Transfer*, Vol.116, 1994, pp.284-295.
- [15] H. Kawamura, H. Abe, Y. Matsuo, DNS of Turbulent Heat Transfer in Channel Flow with Respect to Reynolds and Prandtl Number Effects, *International Journal of Heat and Fluid Flow*, Vol.20, 1999, pp.196-207.